

Glycerol Electrooxidation on Au Supported on Carbon Spheres by Stöber Method in Alkaline Medium

Jian-Hua Zhang, Tao Zhu, Nan Li, Chang-Wei Xu*

Guangzhou Key Laboratory for Environmentally Functional Materials and Technology, School of Chemistry and Chemical Engineering, Guangzhou University, Guangzhou 510006, China

*E-mail: cwxuneuzsu@126.com

Received: 9 May 2013 / *Accepted:* 31 May 2013 / *Published:* 1 July 2013

Carbon spheres (CS) with a size of 500-700 nm were prepared by carbonization resorcinol–formaldehyde polymer spheres which were obtained via the Stöber method. The oxygen-containing functional groups after functionalization by H₂SO₄/HNO₃ mixture act as “glue” to immobilize gold nanoparticles on the surface of functionalized CS (FCS). The gold nanoparticles supported on FCS (Au/FCS) are used for glycerol electrooxidation in alkaline medium. The results show that Au/FCS give better performance than gold nanoparticles supported on carbon black (Au/C). The value of peak current densities on the Au/FCS is 2.7 times higher than that on the Au/C. The gold nanoparticles supported carbon spheres by carbonization resorcinol–formaldehyde polymer spheres via the Stöber method in this paper possess excellent electrocatalytic properties and may be of great potential in direct glycerol fuel cells.

Keywords: Fuel cells; Glycerol; Gold; Carbon spheres; Stöber method

1. INTRODUCTION

Much effort has been devoted to the development of direct alcohol fuel cells (DAFCs) with methanol as fuel [1,2]. However, the development of DAFCs based on methanol fuel is facing serious difficulties: (i) slow electro-kinetic of methanol oxidation, (ii) high methanol crossover and (iii) high toxicity of methanol. Therefore, other alcohols have been considered as alternative fuels. Among various liquid fuels, ethanol is particularly attractive due to its much less toxicity as compared to methanol and abundant availability in great quantities via the fermentation of bio-mass crops such as cereals, sugar beet and maize [3,4]. Pt-based nanoparticles have been extensively investigated and proved as good electrocatalysts for the electrooxidation of methanol and ethanol [5-8]. However, the

high price and limited supply of Pt constitute major barriers to the development of DAFCs. Our previous work on the development of Pt-free electrocatalysts for alcohol oxidation has focused on Pd-based electrocatalysts and the results revealed that Pd is a good electrocatalyst for ethanol oxidation in alkaline medium [9-11]. Other groups have proved the same results [12-15]. Pd-based electrocatalysts are attractive as Pd is at least fifty times more abundant than Pt on the earth. However, the price of Pd is also expensive. Au is paid attention as Au is much more abundant and more available than Pt and Pd on the earth. We have studied the activity and stability of glycerol oxidation on the Au electrode in alkaline medium [16]. The glycerol shows a remarkable activity on the Au electrode. Glycerol has been investigated as the fuel for DAFCs due to high boiling points and non-toxic compared with methanol. Glycerol has higher theoretical energy density than methanol and can be electrochemically oxidized [17-20]. The application of glycerol electrooxidation on DAFCs has attracted increased interest and the DAFCs with glycerol as fuel show certain advantages such as low fuel cross-over and high power density [21-23]. A few of studies have reported the electrocatalytic property of glycerol oxidation on the Au electrode [24-29].

The effect of the supporting material on the catalytic activity of the electrocatalysts for alcohol oxidation is of continued interest. It is well known that carbon materials such as carbon nanotubes, carbon nanofibers and graphene have been used as catalyst support for DAFCs [30-33]. The carbon spheres (CS) have been used as supports for alcohol electrooxidation [9,34-38]. Liu and his cooperators have prepared CS by carbonization resorcinol–formaldehyde (RF) polymer spheres which were obtained via the Stöber method in 2011 [39]. The RF polymer spheres via the Stöber method were firstly reported by Pekala in 1989 [40]. Liu et al. reported firstly the RF polymeric spheres via the Stöber method were transformed to monodisperse CS with uniform and controllable particle size on the submicrometer scale [39]. After loading with platinum nanoparticles, the CS revealed very good electrocatalytic supported materials for oxygen reduction performance [39]. The synthesis approach is a very facile and versatile procedure for making polymer beads and considered to be low cost and suitable for industrial production CS [39]. With this method, Jaroniec and his cooperators have prepared CS as supports for Au to obtain carbon–gold core–shell particles [41]. In this paper, CS were prepared with the same method to support Au nanoparticles for glycerol electrooxidation, as to demonstrate the feasibility of applying CS by carbonization RF polymer spheres via the Stöber method in direct alcohol fuel cell.

2. EXPERIMENTAL DETAILS

CS were prepared by carbonization RF polymer spheres obtained via the Stöber method [39-41]. A mixture with 8 mL ethanol and 20 mL distilled water was maintained at 30°C. Subsequently, 0.1 mL 25 wt% ammonia and 0.2 g resorcinol were added to the above mixture under stirring. Next, 0.28 mL 37 wt% formaldehyde was added to the solution dropwise. After 24 h the mixture was transferred to a Teflon-lined autoclave and placed in an oven for 24 h at 100°C. The precursors were washed and dried at 100°C for 12 h. The precursors in a quartz boat were put into tube furnace for carbonization in a flowing nitrogen atmosphere ($20 \text{ dm}^3 \text{ h}^{-1}$). The temperature program was as follows:

first, the temperature was increased from the room temperature to 350°C with 1°C min⁻¹ heating rate and maintained for 2 h; next, the temperature was increased to 600°C with 1°C min⁻¹ and maintained for 4 h. Finally, the temperature was cooled down to room temperature naturally.

The functionalization of CS was carried out in a 6 mol L⁻¹ H₂SO₄ and 6 mol L⁻¹ HNO₃ solution under constant stirring for 15 min and then refluxed at 80°C for 6 h. The functionalized CS (FCS) were diluted with distilled water and filtered, then washed with excess distilled water to neutral and dried at about 80°C for future use. Au supported on carbon black (Vulcan XC-72, Cabot) and FCS was synthesized at room temperature by chemical reduction using NaBH₄. Excess 0.01 mol L⁻¹ NaBH₄ solution was mixed with the HAuCl₄ solution containing carbon black or FCS under stirring. The resulted material was washed with distilled water and dried at 60°C in vacuum. The working electrode was fabricated by casting polytetrafluoroethylene(PTFE)-impregnated catalyst ink onto a 0.50 cm² carbon rod electrode. The PTFE, gold loading on electrode was 0.10 mg cm⁻². The gold percentage loading was controlled as 20 wt% in electrocatalysts.

All electrochemical measurements were tested in a three-electrode cell using the EG&GPAR283 electrochemical work station (Princeton, USA) in a temperature-controlled water-bath (Polyscience 9106, U.S.A.). Solutions were freshly prepared before each experiment. A platinum foil (3.0 cm²) was used as counter electrode. All the potentials were measured versus a saturated calomel electrode (SCE, 0.241 V *versus* RHE) electrode. A salt bridge was used between the cell and the reference electrode. Fourier transform infrared spectroscopy (FTIR) and Raman analysis were performed on Bruker Tensor 27 and Renishaw inVia. X-ray diffraction (XRD) was carried out with a D/MAX2200 diffractometer. Scanning electron microscopic (SEM) and transmission electron microscopy (TEM) analysis were performed with JSM-7001F scanning electron microscope and JEM-2010HR transmission electron microscope.

3. RESULTS AND DISCUSSION

The structure of CS samples was characterized by Raman spectrum as shown in Fig. 1. The G band peaked at 1595 cm⁻¹ is closely related to a graphitic carbon with a sp² electronic configuration and sensitive to the graphite crystallite component in carbon materials. The D band peak at 1371 cm⁻¹ is assigned to disordered carbon and highly sensitive to graphitic defects within the graphite layers [42]. The intense G peak and the weak D band of the CS suggests that the products have little structure defects and high crystalline quality [43,44]. The ratio of the peak intensity of D band to that of G band (I_D/I_G) is smaller, the degree of crystallinity will be higher. The high integrity of the crystallinity is vital to obtain the conductivity and stability of CS used as electrocatalyst supports.

Fig. 2a and Fig. 2b show the typical SEM and TEM micrographs of CS. It can be observed that the diameter of CS is 500-700 nm. The types of the chemical groups on the surface of CS were characterized by FTIR and the results are shown in Fig. 3. The characteristic bands at 1457 cm⁻¹ are associated with the -CH₂-bending vibrations and scissor vibrations [45]. The absorption bands at 1539 and 1615 cm⁻¹ are assigned to aromatic ring stretching vibrations. The bands at 1249 cm⁻¹ are associated with C-C stretching vibrations. The peaks at 1604 cm⁻¹ are characteristic peaks of C=C

bonds vibrations. After functionalization by $\text{H}_2\text{SO}_4/\text{HNO}_3$ mixture, some additional bands appear in the spectrum of the FCS. The peak at 1716 cm^{-1} is assigned to the $\text{C}=\text{O}$ stretching vibration of carboxyl or carbonyl groups [46]. The broad bands at $3086 \sim 3374\text{ cm}^{-1}$ are attributed to hydroxyl groups stretching vibrations. The results are in agreement with that carbon materials can be functionalized by oxidation of a mixture consisting of $\text{H}_2\text{SO}_4/\text{HNO}_3$ and form the oxygen-containing functional groups, such as $-\text{COOH}$, $-\text{OH}$, etc. [47].

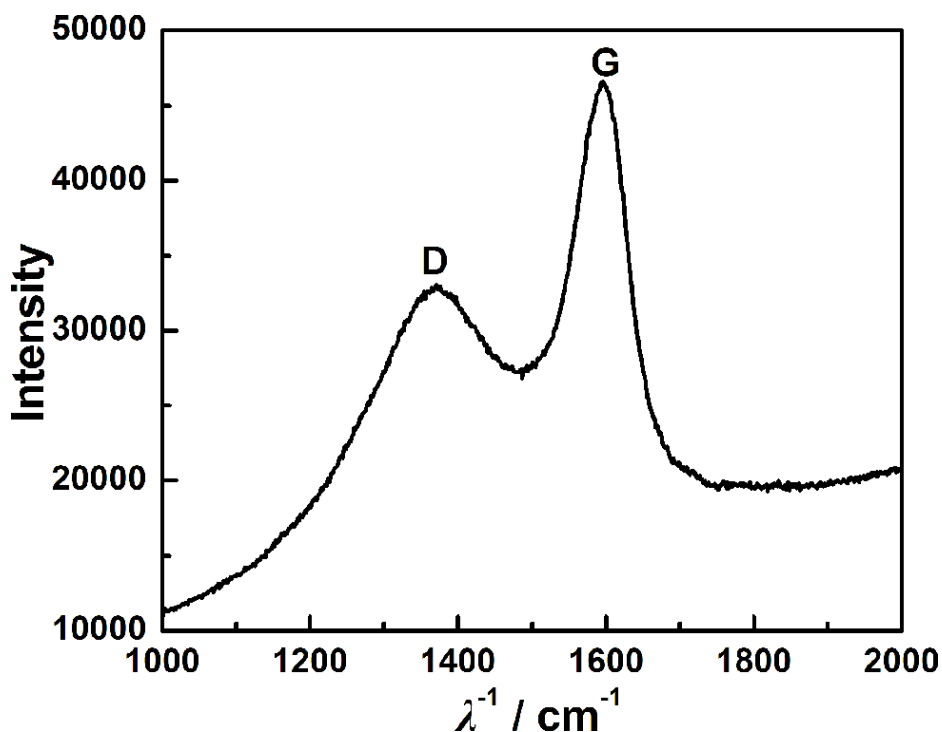


Figure 1. Raman spectrum of CS.

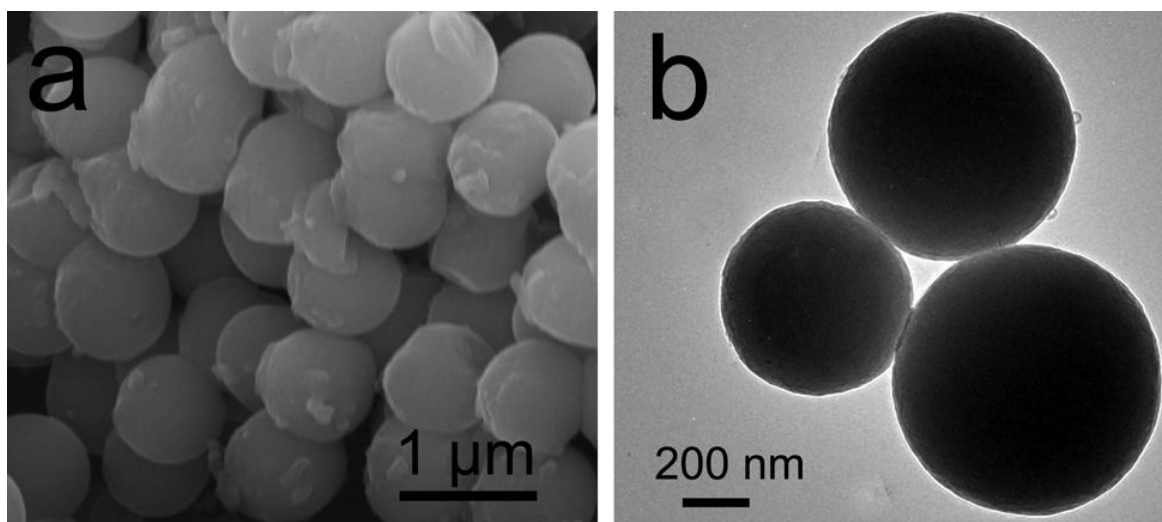


Figure 2. (a) SEM image of CS; (b) TEM image of CS.

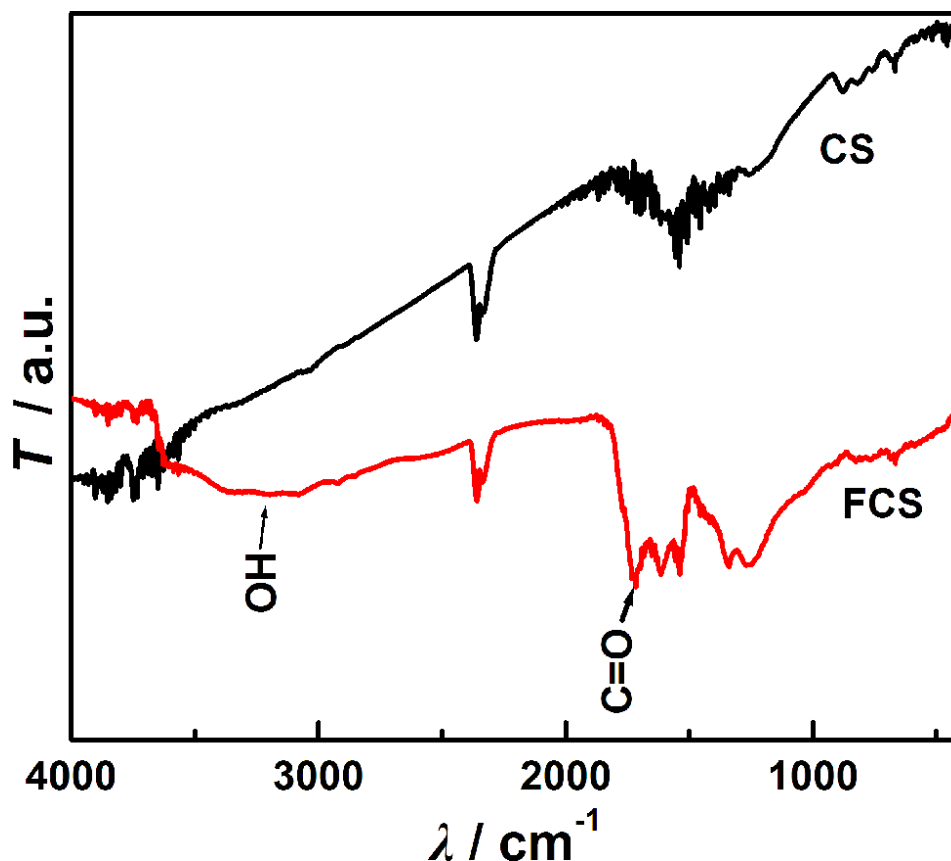


Figure 3. FTIR spectra of CS and FCS.

Fig. 4a is the typical TEM micrograph of gold particles immobilized on CS spheres without any modification. The gold particles can't be immobilized on the surface of those CS without modification. The most Au particles do not disperse on the surface of CS with serious agglomeration. Fig. 4b and Fig. 4c are the typical TEM micrographs of gold particles immobilized on the FCS. The gold particles are immobilized on the outer surface of those FCS in a well-dispersed way. The most Au particles are round and uniformly dispersed on the FCS without agglomeration. The histogram of particle sizes evaluated from over the particles shown in Fig. 4c. The Au average particle size measured from the TEM image is 8.9 nm. The FTIR spectrum of FCS shows that there are many hydroxyl groups with oxygen atoms distributing on the surface of the FCS. Oxygen atoms on FCS can act as "glue" to immobilize gold ions on the surface of FCS could stabilize gold metal. The gold metal atoms were maintained on the outer surface of FCS after reduction. These gold metal atoms tend to coalescence, forming gold nanoparticles. The gold nanoparticles would be ultimately stabilized by a strong bonding interaction between the surrounding oxygen atoms of FCS. The Au/C and Au/FCS exhibit an XRD pattern of a typical face-centered-cubic (fcc) lattice structure as shown in Fig. 5. The strong diffraction peaks at the Bragg angles of 38.1° , 44.3° , 64.5° , 77.5° and 81.6° correspond to the (111), (200), (220), (311) and (222) facets of Au crystal.

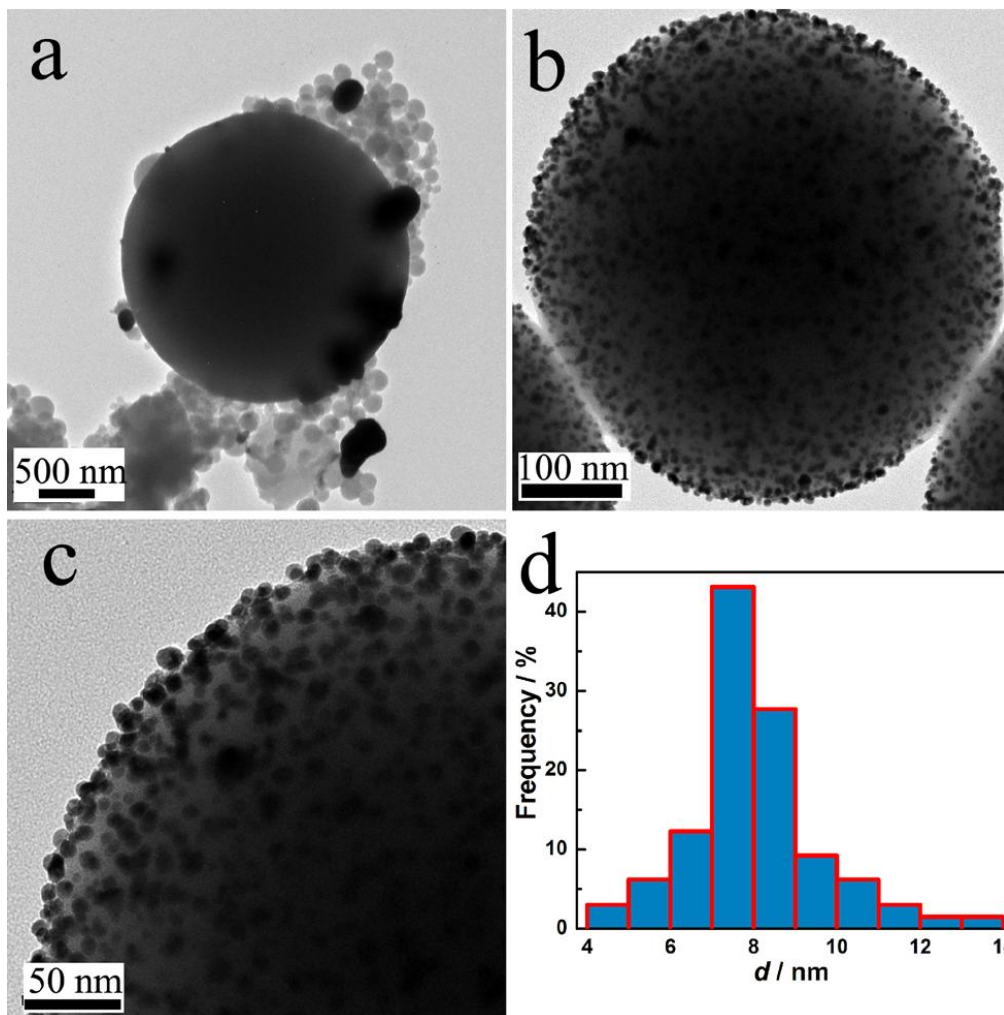


Figure 4. (a) SEM image of Au/CS; (b,c) TEM images of Au/FCS; (d) particle size histogram of Au/FCS.

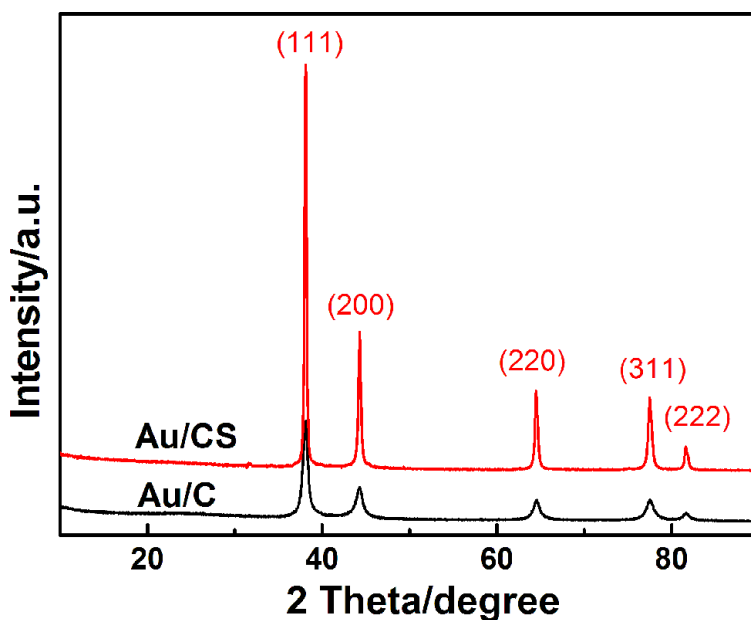


Figure 5. XRD patterns of Au/C and Au/FCS.

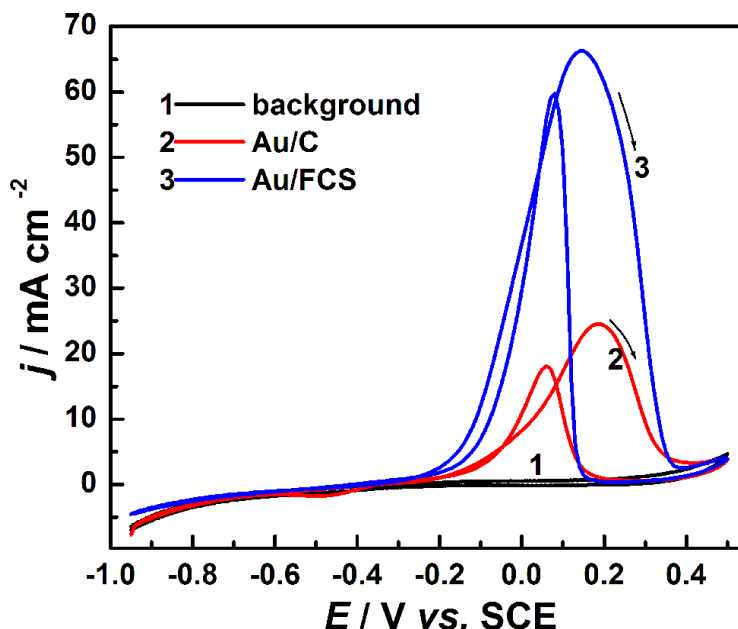


Figure 6. CVs for glycerol electrooxidation on Au/C and Au/FCS electrodes in 1.0 mol L^{-1} glycerol + 1.0 mol L^{-1} KOH with gold loading of 0.10 mg cm^{-2} and a scan rate of 10 mV s^{-1} .

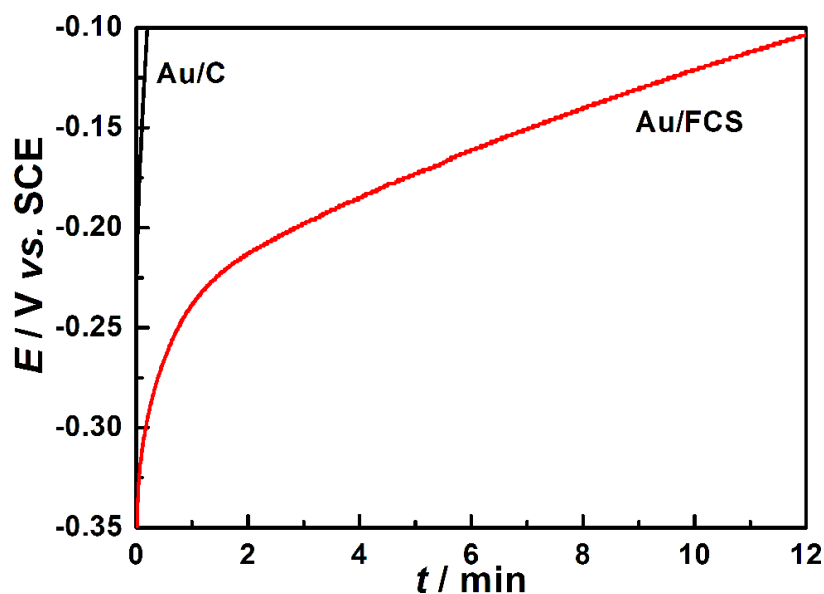


Figure 7. Chronoamperometric curves for glycerol oxidation on Au/C and Au/FCS electrodes in 1.0 mol L^{-1} glycerol + 1.0 mol L^{-1} KOH with gold loading of 0.10 mg cm^{-2} and a fixed current density of 0.3 mA cm^{-2} .

Fig. 6 shows the typical cyclic voltammograms (CVs) for glycerol oxidation on the Au/C and Au/CS electrodes in 1.0 mol L^{-1} KOH + 1.0 mol L^{-1} glycerol with a sweep rate of 10 mV s^{-1} . The background is the CV of Au/FCS electrode in 1.0 mol L^{-1} KOH absence of glycerol. By comparing to the CV in the absence of glycerol, a glycerol oxidation peak can be clearly observed from the onset potential of -0.23 V . The glycerol electrooxidation is characterized by two well-defined current peaks

on the forward and reverse scans. On the forward scan, the oxidation peak is corresponding to the oxidation of fresh glycerol. The peak current densities (j_p) are 24.5 mA cm^{-2} (at the peak potential of 0.18 V) on the Au/C electrode) and 66.2 mA cm^{-2} (at the peak potential of 0.14 V) on the Au/FCS electrode. The value of j_p on the Au/FCS is 2.7 times higher than that on the Au/C. Fig. 7 shows the chronoamperometric curves for glycerol oxidation on the Au/C and Au/FCS electrodes in 1.0 mol L^{-1} KOH solution containing 1.0 mol L^{-1} glycerol with a fixed current density of 0.5 mA cm^{-2} . The potential increases with the polarization time, indicating the poisoning of the Au/C and Au/FCS electrodes. The polarization potential increases sharply on the Au/C electrode compared with that on the Au/FCS electrode. It took 0.2 min for the polarization potential to reach -0.1 V (e.g., the termination voltage for the alcohol oxidation reaction in the present study) for the reaction on the Au/C electrode. However, it's 12.0 min for the polarization potential which reaches to -0.1 V on the Au/FCS electrode under the same current density. The Au/FCS electrocatalysts have a three-dimensional structure which permits liquid alcohol to diffuse into the catalyst layer easily and forms larger three-phase interface, resulting in the high active area and the reduction of liquid sealing effect [48,49].

4. CONCLUSIONS

This study demonstrates the feasibility of applying carbon spheres by carbonization resorcinol-formaldehyde polymer spheres obtained via the Stöber method in direct alcohol fuel cell. The carbon spheres with a diameter of 500-700 nm have little structure defects and high crystalline quality to obtain the conductivity and stability of carbon spheres used as electrocatalyst supports. The gold particles can't be immobilized on the surface of those carbon spheres. The oxygen-containing functional groups such as -COOH, -OH after functionalization by $\text{H}_2\text{SO}_4/\text{HNO}_3$ mixture act as "glue" to immobilize gold nanoparticles on the surface of functionalized carbon spheres (FCS). The gold particles are immobilized in a well-dispersed way on the outer surface of those carbon spheres carbon spheres. The most Au particles are round and uniformly dispersed on the FCS without agglomeration with a size of 8.9 nm. The results show that Au/FCS give better performance for glycerol electrooxidation than gold nanoparticles supported on carbon black (Au/C) in alkaline medium. The values of peak current densities on the Au/FCS are 2.7 times higher than that on the Au/C. The Au/FCS have a three-dimensional structure which permits liquid alcohol to diffuse into the catalyst layer easily and forms larger three-phase interface, resulting in the high active area and the reduction of liquid sealing effect. The gold nanoparticles supported carbon spheres by carbonization resorcinol-formaldehyde polymer spheres via the Stöber method in this paper possess excellent electrocatalytic properties and may be of great potential in direct glycerol fuel cells.

ACKNOWLEDGMENTS

This work was financially supported by the National Natural Science Foundations of China (20903028), Scientific Research Foundation for Returned Scholars from Ministry of Education of China (Xu Changwei), Scientific Research Foundation for Yangcheng Scholar (10A041G), Guangdong Province Natural Science Foundation (s2011040004152) and Guangzhou science and technology plan projects (12C72011619).

References

1. S. Tominaka, S. Ohta, H. Obata, T. Momma and T. Osaka, *J. Am. Chem. Soc.*, 130 (2008) 10456
2. D. Morales-Acosta, D.L. Fuente, L.G. Arriaga, G.V. Gutiérrez and F.J.R. Varela, *Int. J. Electrochem. Sci.*, 6 (2011) 1835
3. W.X. Du, Q. Wang, D. Saxner, N. Deskins, D. Su, J.E. Krzanowski, A.I. Frenkel and X.W. Teng, *J. Am. Chem. Soc.*, 133 (2011) 15172
4. E. Antolini, *J. Power Sources.*, 170 (2007) 1
5. S. J. Liao, K.A. Holmes, H. Tsapralis and V. Birss, *J. Am. Chem. Soc.*, 128 (2006) 3504
6. N. Tian, Z.Y. Zhou, S.G. Sun, Y. Ding and Z.L. Wang, *Science*, 316 (2007) 732
7. H.Y. Sun, L.H. Zhao and F.C. Yu, *Int. J. Electrochem. Sci.*, 8(2013)2768-2777
8. L.X. Ding, A.L. Wang, G.R. Li, Z.Q. Liu, W.X. Zhao, C.Y. Su and Y.X. Tong, *J. Am. Chem. Soc.*, 134 (2012) 5730
9. C.W. Xu, L.Q. Cheng, P.K. Shen and Y.L. Liu, *Electrochem. Commun.*, 9 (2007) 997
10. C.W. Xu, P.K. Shen and Y.L. Liu, *J. Power Sources*, 164 (2007) 527
11. C.W. Xu, H. Wang, P.K. Shen and S.P. Jiang, *Adv. Mater.*, 19 (2007) 4256
12. C. Bianchini and P.K. Shen, *Chem. Rev.*, 109 (2009) 4183
13. L. An and T.S. Zhao, *Energy Environ. Sci.*, 4 (2011) 2213
14. N. Tian, Z.Y. Zhou, N.F. Yu, L.Y. Wang and S.G. Sun, *J. Am. Chem. Soc.*, 132 (2010) 7580
15. A. Kowal, M. Li, M. Shao, K. Sasaki, M.B. Vukmirovic, J. Zhang, N.S. Marinkovic, P. Liu, A.I. Frenkel and R.R. Adzic, *Nat. Mater.*, 8 (2009) 325
16. J.H. Zhang, Y.J. Liang, N. Li, Z.Y. Li, C.W. Xu and S.P. Jiang, *Electrochim. Acta*, 59 (2012) 156
17. Y. Kwon and M. Koper, *Anal. Chem.*, 82 (2010) 5420
18. A. Falase, M. Main, K. Garcia, A. Serov, C. Lau and P. Atanassov, *Electrochim. Acta*, 66 (2012) 295
19. K. Matsuoka, M. Inaba, Y. Iriyama, T. Abe, Z. Ogumi and M. Matsuoka, *Fuel Cells*, 2 (2002) 35
20. C.C. Jin, Z. Zhang, Z.D. Chen and Q. Chen, *Int. J. Electrochem. Sci.*, 8 (2013) 4215
21. Z.Y. Zhang, L. Xin and W.Z. Li, *Appl. Catal. B*, 119 (2012) 40
22. A. Ile, M. Simoes, S. Baranton, C. Coutanceau and S. Martemianov, *J. Power Sources*, 196 (2011) 4965
23. M. Simões, S. Baranton and C. Coutanceau, *Electrochim. Acta*, 56 (2010) 580
24. D.Z. Jeffery and G.A. Camara, *Electrochem. Commun.*, 12 (2010) 1129
25. Y. Kwon, S.C.S. Lai, P. Rodriguez and M.T.M. Koper, *J. Am. Chem. Soc.*, 133 (2011) 6914.
26. S. Yongprapat, A. Therdthianwong and S. Therdthianwong, *J. Appl. Electrochem.*, 42 (2012) 483
27. Z.Y. Zhang, L. Xin and W.Z. Li, *Int. J. Hydrogen Energ.*, 37 (2012) 9393
28. J.H. Song, J.Y. Yu and C.W. Xu, *Int. J. Electrochem. Sci.*, 7 (2012) 4362
29. J.H. Song, S.J. Fan, J.Y. Yu, K.H. Ye and C.W. Xu, *Int. J. Electrochem. Sci.*, 7 (2012) 10842
30. T. Hyeon, S. Han, Y.E. Sung, K.W. Park and Y.W. Kim, *Angew. Chem. Int. Edit.*, 115 (2003) 4488
31. M.M. Zhang, Z.X. Yan and J.M. Xie, *Electrochim. Acta*, 77 (2012) 237
32. P.S. Fernández, M.E. Martins and G.A. Camara, *Electrochim. Acta*, 66 (2012) 180
33. R.H. Wang, Y. Xie, K.Y. Shi, J.Q. Wang, C.G. Tian, P.K. Shen and H.G. Fu, *Chem-Eur. J.*, 18 (2012) 7443
34. Z. Hamoudi, M.A.E. Khakani and M. Mohamedi, *Electroanal.*, 23 (2011) 1205
35. P.K. Shen, Z.X. Yan, H. Meng, M.M. Wu, G.F. Cui, R.H. Wang, L. Wang, K.Y. Si and H.G. Fu, *RSC Adv.*, 1 (2011) 191
36. Z. Hamoudi, B. Aissa, M.A.E. Khakani and M. Mohamedi, *J. Phys. Chem. C*, 114 (2010) 1885
37. Y.C. Liu, X.P. Qiu, Y.Q. Huang and W.T. Zhu, *Carbon*, 40 (2002) 2375
38. C.W. Xu, Y.L. Liu and D.S. Yuan, *Int. J. Electrochem. Sci.*, 2 (2007) 674

39. J. Liu, S.Z. Qiao, H. Liu, J. Chen, A. Orpe, D. Zhao and Q.G. Liu, *Angew. Chem. Int. Edit.*, 50 (2011) 5947
40. R.W. Pekala, *J. Mater. Sci.*, 24 (1989) 3221
41. J. Choma, D. Jamiola, K. Augustynek, M. Marszewski and M. Jaroniec, *Chem. Commun.*, 48 (2012) 3972
42. R.V. Hull, L. Li, Y. Xing and C.C. Chusuei, *Chem. Mater.*, 18 (2006) 1780
43. A. Kaniyoor, T.T. Baby and S. Ramaprabhu, *J. Mater. Chem.*, 20 (2010) 8467
44. M.Z. Liu, Y. Yan, L. Zhang, X. Wang and C. Wang, *J. Mater. Chem.*, 22 (2012) 11458
45. L. Zhang, H.B. Liu, M. Wang and L. Chen, *Carbon*, 45 (2007) 1439
46. Y. H. Qin, H.H. Yang, X.S. Zhang, P. Li, X.G. Zhou, L. Niu and W.K. Yuan, *Carbon*, 48 (2010) 3323
47. X.H. Li, J.L. Niu, J. Zhang, H.L. Li and Z.F. Liu, *J. Phys. Chem. B*, 107 (2003) 2453
48. F.Y. Xie, H. Meng and P.K. Shen, *Electrochim. Acta*, 53 (2008) 5039
49. Z.X. Yan, H. Meng, P.K. Shen, Y.Z. Meng and H.B. Ji, *Int. J. Hydrogen Energ.*, 37 (2012) 4728